Cellulose (2017) 24:2469–2481
DOI 10.1007/s10570-017-1273-2

ORIGINAL PAPER

Understanding the effect of synthesis parameters on the catalytic ionic liquid hydrolysis process of cellulose nanocrystals

Nurul Atikah Mohd Iskak · Nurhidayatullaili Muhd Julkapli · Sharifah Bee Abdul Hamid

Received: 19 October 2016 / Accepted: 27 March 2017 / Published online: 3 April 2017

Abstract Conventional production of cellulose nanocrystals (CNC) normally encounters several problems including high energy consumption, toxicity and corrosion risk. Implementation of green solvent ionic liquid (IL) is an alternative to this conventional method. Production of CNC is known to be influenced by several factors such as reaction time and temperature. However, limited studies on the regeneration yield and other properties of CNC produced at both variables can be found. In this paper, CNC with desirable yield, crystallinity and particle size has been produced under catalytic hydrolysis process of IL. Two different parameters have been studied which are reaction temperature and time. It was found that, CNC with particle size of 9 nm and 73% crystallinity index has been produced at 30 min reaction time. Meanwhile, 100 °C reaction temperature manages to produce CNC with 90% yield and 76% crystallinity. In conclusion, reaction temperature and time affect the yield and thermal properties of hydrolysis process.

Keywords Cellulose · Ionic liquid · Crystallinity · Yield · Temperature · Reaction time

N. A. M. Iskak · N. M. Julkapli (✉) · S. B. A. Hamid
Nanotechnology and Catalysis Research Center (NANOCAT), Level 3, Block A, Institute of Postgraduate Studies, University of Malaya, 50603 Kuala Lumpur, Malaysia
e-mail: nurhidayatullaili@um.edu.my

Introduction

Over the past decades, several methods have been developed in cellulose nanocrystals (CNC) production. For example, cryocrushing methods required frozen and high shear forces condition which in turn increase the cost and alter the crystallinity properties of CNC. However, a major obstacle that needs to be overcome is the high energy consumption connected to the mechanical disintegration of the cellulose to CNC. On the other hand, the use of concentrated mineral acids is efficient at high temperature (170–240 °C). In enzymatic hydrolysis, the obvious disadvantages are low activity, high cost of enzymes and separation problems because of the solubility in water. Compared to acid hydrolysis, enzymatic hydrolysis is a cleaner and more selective process that takes place at moderate pressures and temperatures. However, acid hydrolysis of cellulose occurs at a faster rate and the acids used are cheaper than the enzymes. The drawback of acid hydrolysis is its high processing temperature, a condition which raises the cost of the equipment and increases the corrosion (Camacho et al. 1996). In the sub- or supercritical water methods, cellulose is treated in the absence of catalysts at 200–400 °C and above 20 MPa with low selectivity. Supercritical water has recently been used as a medium for hydrolysis of cellulose, but harsh conditions such as high temperature and pressure mentioned before were required. Knowing the above disadvantages, a new, green and economical process

for the formation of CNC is developed as an alternative to the conventional methods.

With increasing governmental regulations in industries, implementation of "green" process is an alternative especially for preventing pollution and acting as a strong driving force to discover effective solvents in producing CNC (Zhang et al. 2005). Ionic liquids (ILs), which are also referred to as room temperature ionic liquids, room temperature molten salts, organic ionic liquids, etc. refer to an ionic system which takes on a liquid state at the room temperature or slightly warmer (Feng et al. 2008). ILs are a class of highly polar solvents that are entirely constituted of ions (Cheng and Chu 2006). The salient characteristics distinguishing ILs from conventional solvents are the wide range of melting temperature (−40 to 400 °C), high thermal stability (up to 400 °C), weakly coordinating properties, low flammability, high conductivity (both ionic and thermal), broad electrochemical potential window (−4 to 4 V) and low vapour pressure, which minimizes the risk to the workers by exposure to volatile fumes observed with other chemical pretreatments (Olivier-Bourbigou et al. 2010). Different studies on production of CNC using two most common ILs, 1-butyl-3-methylimidazolium hydrogen sulphate [Bmim][HSO4] and 1-butyl-3-methylimidazolium chloride [Bmim][Cl] has been conducted previously. It was found that CNC produced by ILs have high crystallinity index up to 96% (Tan et al. 2015). However, there is still limited findings on the regeneration yield and thermal properties of CNC produced by ILs so more focussed study is needed. Thus, this study was conducted in order to investigate the effect of reaction temperature and time on the properties of NCC synthesized using [Bmim][Cl]. In this study, microcrystalline cellulose (MCC) was chosen as the material to study since it is readily characterized. MCC was dissolved into 1-butyl-3-methylimidazolium chloride ([Bmim][Cl]) at different temperature (40, 60, 80 and 100 °C) and reaction time (30, 60, 90 and 120 min). Resulting cellulose/([Bmim] Cl) mixture was then separated by adding water as an anti-solvent, where the precipitate cellulose samples were characterized by Atomic Force Microscopy (AFM), X-ray diffraction (XRD), Fourier Transform Infrared Spectroscopy (FTIR) and Differential Scanning Calorimetry (DSC) and regeneration yield.

Experimental

Materials

MCC (Friendemann Schmidt) with an average particle diameter of 2–20 μm was purchased. The MCC was confirmed to be Cellulose I by X-ray diffraction patterns and the crystallinity index was 60% calculated by Segal method (Segal et al. 1959). 1-butyl-3-methylimidazolium chloride ([Bmim][Cl]) of analytical grade was purchased from Merck and used without further purification. Deionized water (Millipore) was used throughout this work.

Methods

Hydrolysis was carried out using [Bmim]Cl solvent at two different parameters: (1) reaction temperature (40, 60, 80, 100 °C), (2) reaction time (30, 60, 90 and 120 min) under 400 rpm mechanical stirring. The reaction was quenched by adding deionized water. The resulting suspensions was sonicated and washed by repeated centrifugation. The sediment was freeze-dried before characterization.

Characterization

Yield The effect of preparation conditions on CNC's yield was gravimetrically determined in following step. After separation of the CNC using a centrifuge at 7000 rpm for 30 min, the CNC was dried and weighed. The CNC yield was determined as a percentage of dry weight of the "starting" material. Total yield of CNC was calculated as follows:

$$\mathrm{Y},\ \% = 100\,(\mathrm{W}/\mathrm{W}_0), \tag{1}$$

where W_0 is the initial dry weight of the sample and W is the weight of dried sediment.

Fourier transform infrared spectroscopy (FTIR) FTIR was employed to examine the changes in the chemical composition of cellulose after treatment. MCC and the CNC were analyzed. Infrared spectra were measured with diffuse reflectance (Bruker—IFS 66) between 4000–400 cm^{-1}, with a resolution of 4 cm^{-1} and 16 times of scans. Dried samples were mixed with KBr powder using an agate mortar.

Thermogravimetric analysis (TGA) TGA could stipulate detailed information on the change of mass of a sample as a function of temperature, whereby in the presence of inert gases, the loss of mass was credited to the loss of volatile matter and decomposition as a function of temperature. Information of separate constituents within the lignocellulosic biomass based on their temperature response and rate of volatilization/decomposition was obtainable from the TGA. The thermal stability of the CNC was characterized using thermogravimetric analysis (TGA) (Mettler Toledo, TGA/SDTA 851) model. Approximately 5 mg of each sample was heated from room temperature to 700 °C at a heating rate of 10 °C/min under nitrogen atmosphere.

Atomic force microscopy (AFM) The morphology and diameter of CNC samples were investigated by using atomic force microscopy (AFM). Samples were prepared by dispersing CNC in distilled water in an ultrasonic bath at room temperature for 1 h, in order to loosen up the cellulose particles. A droplet of the resulting solution was cast onto cleaved mica and dried under ambient conditions. The samples were then analyzed with a scanning probe microscope. Optical micrographs were analyzed using Nanoscope Analysis 1.5 software in order to determine the average diameter and length of CNC.

X-ray diffractometry (XRD) X-ray diffraction measurements were conducted using D8 Advance, Bruker AXS model system equipped with Cu Kα radiation ($\lambda = 0.154$ nm) at 40 kV and 40 mA in range of 5°–40° at 0.01° interval with fixed time method. The crystallinity is defined as the ratio of the amount of crystalline cellulose to the total amount of sample material, including crystalline and amorphous parts. The crystallinity index (CrI) was calculated using Segal's method as follows: (Segal et al. 1959)

$$\mathrm{CrI}\ (\%) = \frac{I_{200} - I_{AM}}{I_{200}} \times 100\% \qquad (2)$$

where I_{200} is the height of the 200 peak, which represents both crystalline and amorphous material; I_{AM} is the lowest height between the 200 and 110 peaks, which represents amorphous material only.

Results and discussions

Effect of temperature

Yield

The effect of temperature on structure and size of CNC was preliminary studied at different heating temperature (40, 60, 80 and 100 °C). In previous study, heat is a well-known assisted treatment applied for enhancing the dissolution of cellulose in ILs. The heat applied was normally between 45 °C up to 160 °C (Montalbo-Lomboy and Grewell 2015). In another study by Hong et al. (2002), it was reported that [Bmim]Cl reaction only require a mild heat treatment to dissolve cellulose Thus, this study has narrowed the temperature range to 40–100 °C in order to minimize the energy consumption and avoiding cellulose degradation. For all cellulose treatment, the maximum yield of CNC has always been a critical challenge. After hydrolysis at different temperature;

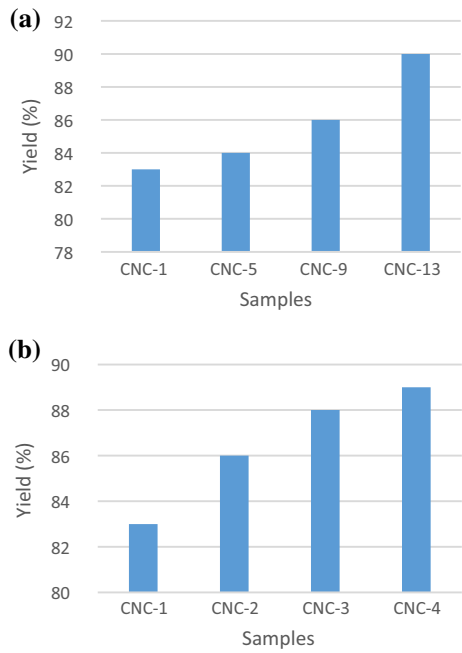

Fig. 1 Yield of CNC at **a** increasing temperature (CNC-1 = 40 °C, CNC-5 = 60 °C, CNC-9 = 80 °C and CNC-13 = 100 °C) and **b** reaction time (CNC-1 = 30 min, CNC-2 = 60 min, CNC-3 = 90 min and CNC-4 = 120 min)

40, 60, 80 and 100 °C, the results are presented in Fig. 1a.

The CNC yields were 83, 84, 86 and 90% (CNC-1, CNC-5, CNC-9 and CNC-13) from ILs hydrolysis at 40, 60, 80 and 100 °C, respectively. The yields increased significantly by 1, 2 and 4% with increasing temperature, validating the effectiveness of higher temperature. This showed that the reaction rate was improved as the temperature was increased. Results showed that the CNC production was very efficient at maximum reaction temperature, giving 90% yield at 2 h treatment time. As reported by Remsing et al. (2006), cellulose was dissolved into ILs because the chloride ions in ILs could go into the interspaces of 1,4-linked β-D-glucose units and disrupt intermolecular hydrogen bonds between the units (Hu et al. 2013). Supposedly, when the temperature was increased, [Bmim]Cl became less viscous, which would enhance the movement rate of chloride ions and then accelerate the dissolution of cellulose and improve the yield of CNC. Contrary with the previous research, it was found that more cellulose was recovered at 90 °C compared to 120 °C. This was probably related to the excessive degradation of cellulose at temperature higher than 100 °C. Compared with conventional method, using ILs was proven to be more efficient in producing high yield of cellulose as only 21–38% of CNC can be recovered at the temperature of 65 °C, by using sulphuric acid (Brinchi et al. 2013).

X-ray diffractometry (XRD)

To give more detailed information about the effect of ILs hydrolysis of MCC at different reaction time (40, 60, 80 and 100 °C), the x-ray diffractometry (XRD) analysis was used to determine the crystallinity index (CrI) of obtained CNC. The X-ray diffractograms of MCC and extracted CNC are shown in Fig. 2a, which exhibited similar diffraction peaks with four diffraction peaks at $2\Theta = 14$, 16, 22 and 34°.

After treatment at four different temperatures, the cellulose I structure remains for all four samples. For untreated and treated samples, the (200) peak position and peak width stays essentially the same. Naturally, cellulose consists of highly ordered crystalline domains along with some disordered (amorphous) domains. The highly crystalline domains are known to be resistant to hydrolysis compared to amorphous domains. Within the adequate temperature (40–100 °C) and time (30–120 min), only amorphous domains were removed compared to previous study by Zhang et al. (2014), whereby wider range of temperature and time were used (50–130 °C, 6 h) resulting in lower crystallinity index as crystalline domains were also removed (Zhang et al. 2014). Subsequently, formation of Cellulose II will take place as cellulose is being regenerated. In our study, the crystalline structure of MCC was maintained in CNC due to the adequate conditions used, which controlled the crystallinity index of cellulose from decreasing and

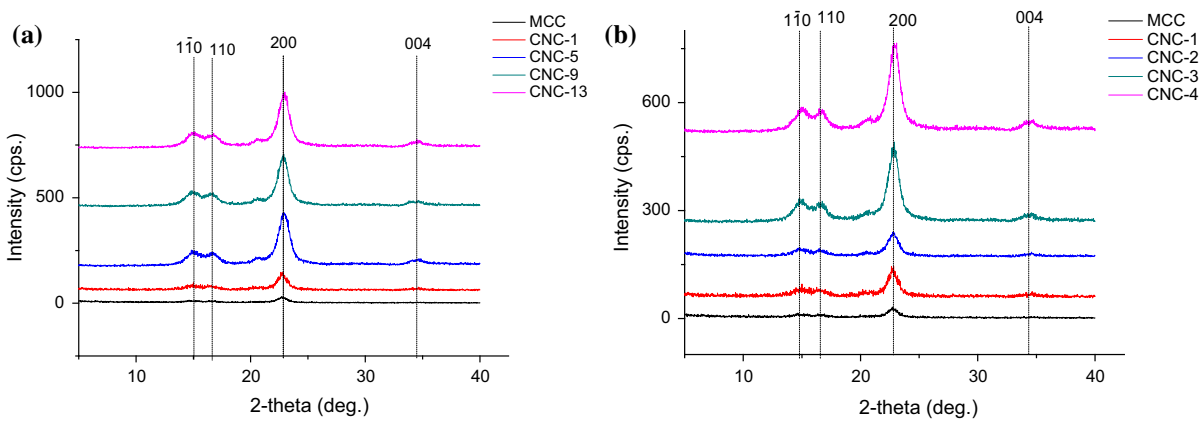

Fig. 2 XRD diffractograms of CNC at **a** increasing temperature (CNC-1 = 40 °C, CNC-5 = 60 °C, CNC-9 = 80 °C and CNC-13 = 100 °C) and **b** reaction time (CNC-1 = 30 min, CNC-2 = 60 min, CNC-3 = 90 min and CNC-4 = 120 min)

regenerated as another cellulose structure. An investigation on the effect of temperature on crystallinity of CNC shows increasing trend as can be observed from the Table 1.

A similar observation has been reported for ILs treated sample too (Man et al. 2011). The crystallinity index obtained from X-ray diffractograms for MCC and extracted CNC at 40, 60, 80 and 100 °C was found to be 60, 73, 75, 75 and 76% respectively. Increased CrI of CNC synthesized at 40 °C from MCC was probably due to realignment of crystalline structure, after removing the amorphous domains. Further increase of temperature at 60 °C enhancing more realignments to occur, thus increasing the crystallinity index of the CNC. In previous study, MCC was hydrolysed in 1-butyl-3-methylimidazolium sulphate to yield CNC of high crystallinity, however, this CNC showed to have low crystallinity index, due to the presence of sulphate ion (Brinchi et al. 2013). In this study, the crystalline structure seems to not be affected due to the adequate time used in dissolving cellulose (30–120 min) was probably the other reason since excessive treatment can change the metastable structure of Cellulose I to other derivatives (Cellulose II, III, IV) besides reducing the crystallinity index.

Table 1 Crystallinity index of CNC at increasing temperature (CNC-1 = 40 °C, CNC-5 = 60 °C, CNC-9 = 80 °C and CNC-13 = 100 °C)

Sample	Crystallinity index (%)
MCC	60
CNC-1	73
CNC-5	75
CNC-9	75
CNC-13	76

Thermogravimetric Analysis (TGA)

Results of the thermal behaviour of CNC-1, CNC-5, CNC-9 and CNC-13 are presented in Table 2. The initial mass loss can be ascribed to the evaporation of moisture from cellulose materials. The chemisorbed water was found to be given off at a temperature of 60 °C for all four samples.

In the thermal analysis for CNC-1, CNC-5, CNC-9 and CNC-13, cellulose decomposition started at 330, 340, 350 and 352 °C, respectively. At 700 °C almost all cellulose was pyrolyzed, and the residue mass were relatively small (8, 11, 15, 12%) for CNC-1, CNC-5, CNC-9 and CNC-13, respectively. Based on the TGA and DTG curves in Fig. 3, the thermal decomposition peaks of the maximum mass loss appeared at 350, 370, 380 and 384 °C for CNC-1, CNC-5, CNC-9 and CNC-13, respectively.

Atomic force microscopy

Table 3 shows the diameter, length and aspect ratio of CNC synthesized at different temperature (40, 60, 80 and 100 °C). On average, the CNC are 155, 290, 451, 769 nm long, 9, 20, 30, 33 nm wide and aspect ratio of 17, 14, 15, 23 for CNC-1, CNC-5, CNC-9 and CNC-13, respectively.

As can be seen in Table 3, the diameter and length of CNC increased as the reaction temperature was increased. Analysis of the obtained result revealed a relation between regeneration yield and the morphological properties of CNC. Figure 4a shows AFM images of CNC obtained at four different temperatures.

Table 2 Thermal stability of CNC at increasing temperature (CNC-1 = 40 °C, CNC-5 = 60 °C, CNC-9 = 80 °C and CNC-13 = 100 °C)

Sample	25–150 °C		150–700 °C			Residue mass (%)
	Mass loss (%)	T_1 (°C)	Onset (°C)	Mass loss (%)	T_{max} (°C)	
CNC-1	1.5	60	330	90	350	8
CNC-5	2.0	60	340	87	370	11
CNC-9	0.8	60	350	84	380	15
CNC-13	2.6	60	352	85	384	12

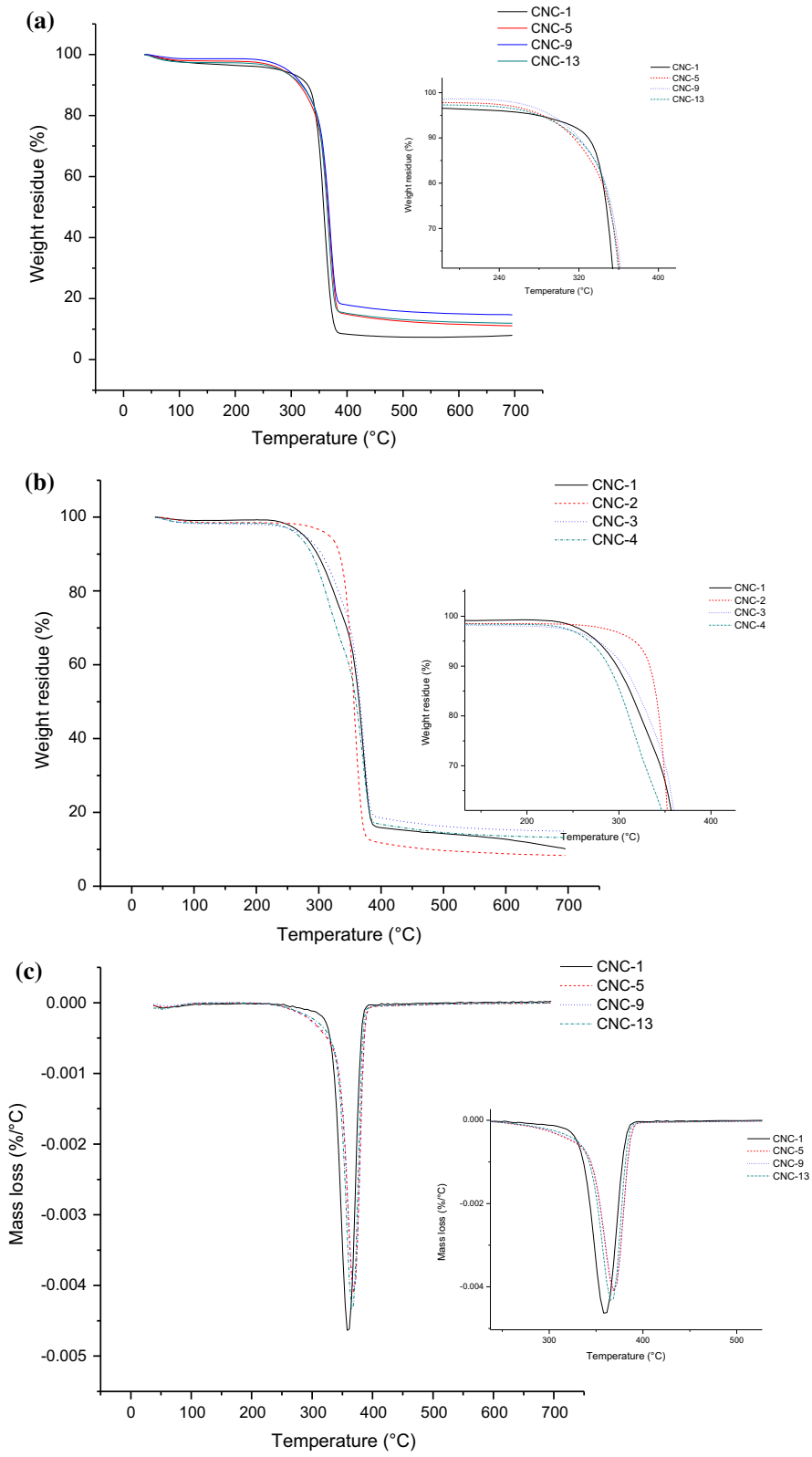

Fig. 3 TGA of NCC at **a** increasing temperature, **b** increasing reaction time and DTG curve of NCC at **c** increasing temperature, **d** increasing reaction time

Fig. 3 continued

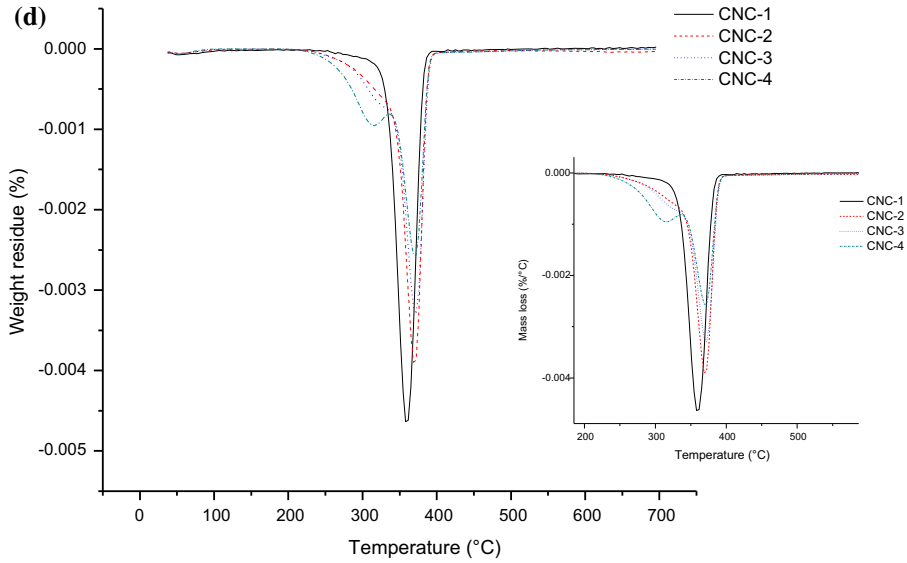

Table 3 Diameter (nm), Length (nm) and aspect ratio of CNC at increasing temperature (CNC-1 = 40 °C, CNC-5 = 60 °C, CNC-9 = 80 °C and CNC-13 = 100 °C)

Sample	Diameter (nm)	Length (nm)	Aspect ratio
CNC-1	9	155	17
CNC-5	20	290	14
CNC-9	30	451	15
CNC-13	33	769	23

The sample with the smallest size of CNC aggregates was 9 nm, obtained with lowest reaction temperature (40 °C). The low standard deviation obtained confirms the accuracy and precision of the method use. Aside from the rod-like structure seen in the micrographs, the diameter of CNC was increased at increasing reaction time, indicating aggregation of the CNC probably due to moisture evaporation during sample preparation. CNC-13 has the highest aspect ratio (23) among four samples (CNC-1, CNC-5, CNC-9, CNC-13). Theoretically, CNC with higher aspect ratio will have higher mechanical strength (Yang et al. 2013).

Fourier transform infrared spectroscopy (FTIR)

FTIR spectroscopy portrays a comparatively simple method of acquiring direct information on chemical changes occurring during various chemical treatments, hence the extensive use in cellulose research (Mandal et al. 2011). The efficiency of each chemical treatment was confirmed by FTIR. Figure 5a, b show the FTIR spectra recorded after hydrolysis with different dissolution time and temperature.

All the spectra were characterized by a dominant O–H stretch band (3345–3348 cm^{-1}) and a C–H stretch band (2903–2906 cm^{-1}) corresponding to the aliphatic moieties in polysaccharides. The band at 1639–1643 cm^{-1} was accredited to the bending mode of the absorbed water. The bands at 1431–1433 cm^{-1} in the spectrum were assigned to the symmetric CH_2 bending, while the C–H bending occurred at 1371–1372 cm^{-1}. Absorption band at 1158 cm^{-1} denotes C–O–C stretching at the β-(1,4)-glycosidic linkages. The in-plane ring stretching gave a shoulder at 1113–1115 cm^{-1}. Strong peak at 1058–1059 cm^{-1} was indicative of C–O stretching at C-3. A small peak at 667–668 cm^{-1} corresponded to the out-of-plane bending of C–O–H. A medium peak at 2900–2906 cm^{-1} was due to C–H stretching. A band in the range within 1643–1646 cm^{-1} was associated with the adsorbed water. The bands at 1329–1330 and 1431–1433 cm^{-1} were assigned to C–C/C–O skeletal vibrations and CH_2 symmetric bending respectively. The sharp bend at 1369–1378 cm^{-1} reflects C–H asymmetric deformation of cellulose. The absorption band at 1163 cm^{-1} corresponds to C–O antisymmetric bridge stretching of cellulose. The absorption bands at 1113–1115 and 1057–1058 cm^{-1} correspond to C–O–C pyranose ring skeletal vibration of cellulose. The absorption band at 894 cm^{-1} corresponds to

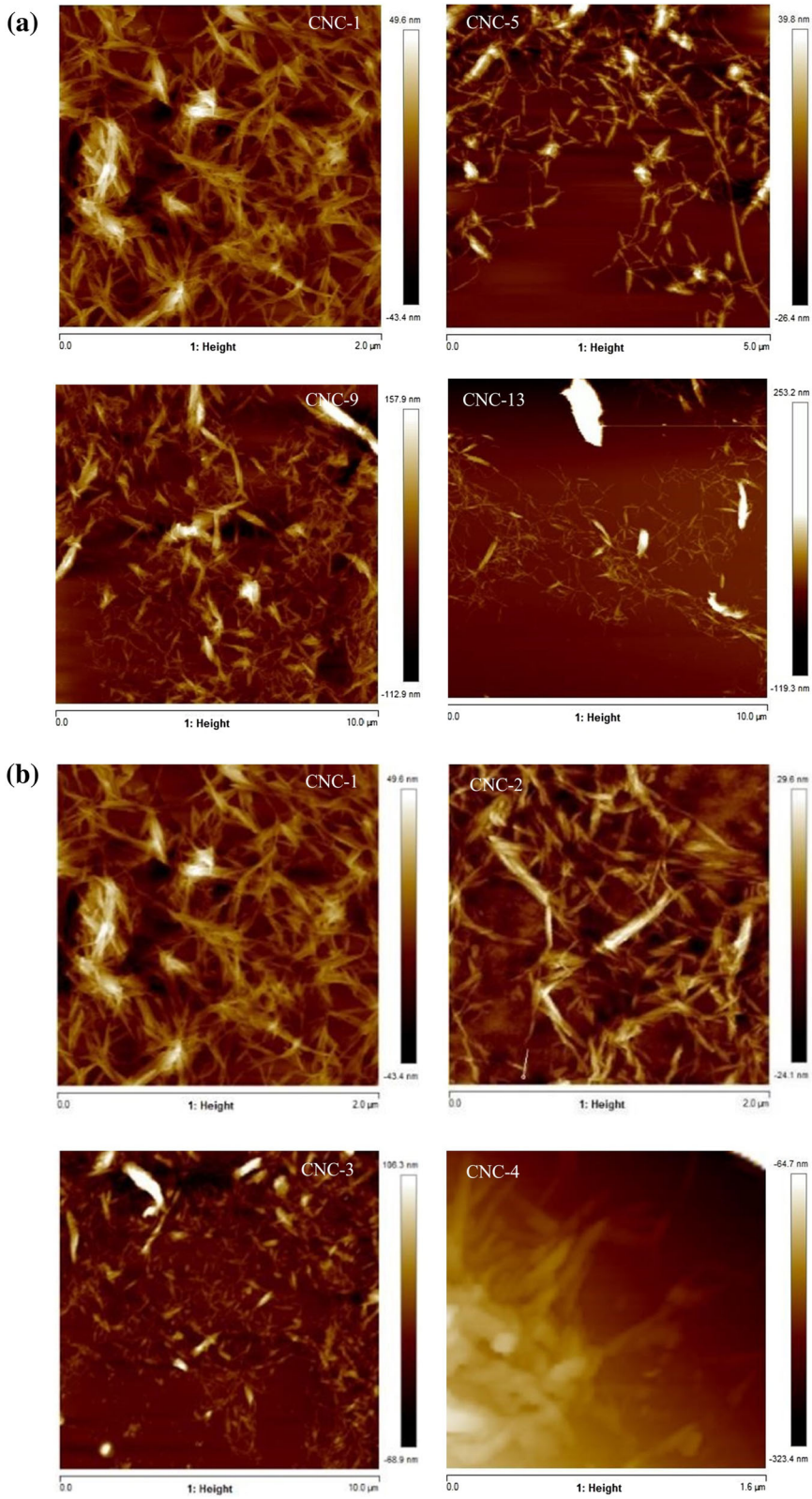
(a)
CNC-1
49.6 nm
-43.4 nm
0.0
1: Height
2.0 µm
CNC-5
39.8 nm
-26.4 nm
0.0
1: Height
5.0 µm
CNC-9
157.9 nm
-112.9 nm
0.0
1: Height
10.0 µm
CNC-13
253.2 nm
-119.3 nm
0.0
1: Height
10.0 µm
(b)
CNC-1
49.6 nm
-43.4 nm
0.0
1: Height
2.0 µm
CNC-2
29.6 nm
-24.1 nm
0.0
1: Height
2.0 µm
CNC-3
196.3 nm
-88.9 nm
0.0
1: Height
10.0 µm
CNC-4
-64.7 nm
-323.4 nm
0.0
1: Height
1.6 µm

◀ **Fig. 4** AFM images of CNC at **a** increasing temperature (CNC-1 = 40 °C, CNC-5 = 60 °C, CNC-9 = 80 °C and CNC-13 = 100 °C) and **b** reaction time (CNC-1 = 30 min, CNC-2 = 60 min, CNC-3 = 90 min and CNC-4 = 120 min)

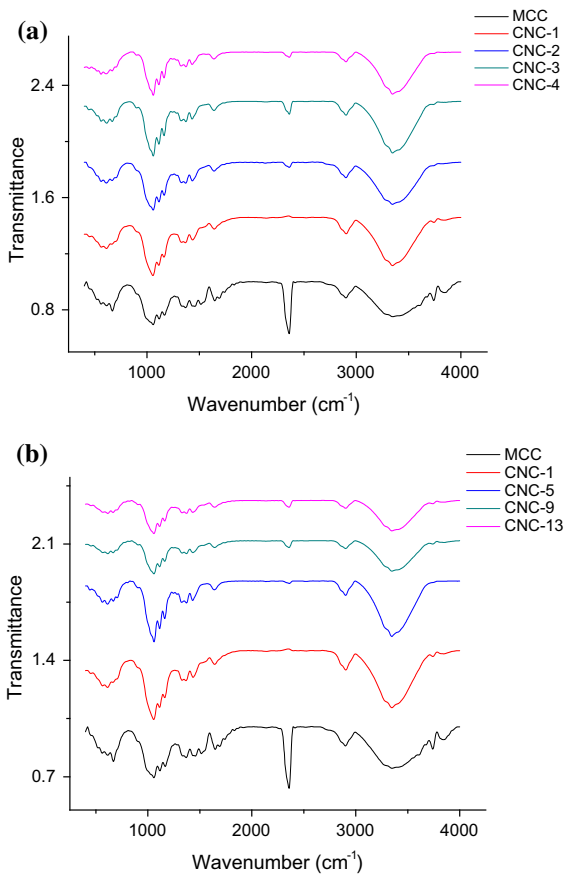

Fig. 5 FTIR spectra of CNC at different **a** reaction time **b** temperature

C–H rocking vibrations of cellulose. FTIR analysis showed that both untreated MCC and CNC obtained after treatment with [Bmim][Cl] have the same basic structure as shown in Fig. 5.

Effect of reaction time

Yield

The effect of reaction time on structure and size of CNC was preliminary studied at different reaction time (30, 60, 90, 120 min) under constant conditions of 40 °C heating temperature (minimum temperature) to avoid severe degradation of cellulose since [Bmim]Cl required only mild heat treatment. In previous study, although degradation of cellulose in [Bmim]Cl was not shown, excessive degradation of cellulose was shown at higher temperature (Zhao et al. 2009). Figure 1b shows the yield of CNC at four different reaction time. The CNC yields were 83, 86, 88 an 89% (CNC-1, CNC-2, CNC-3 and CNC-4) from ILs hydrolysis for 30, 60, 90 and 120 min, respectively. The yields increased by 3, 2 and 1% with the additional times, validating the effectiveness of longer reaction time. This was probably due to formation of total reducing sugars (TRS) or glucose at shorter reaction time. As mentioned in previous research, at higher temperature such as 170 and 180 °C, longer reaction time favoured neither TRS nor glucose formation, whereas the shorter reaction time produced more TRS and glucose (Tian et al. 2010). Also, since the low temperature is used (40 °C), longer time required for the reaction process to achieve optimum yield. The 89% yield of CNC-4 shows that the ILs hydrolysis for as long as 120 min is optimum in releasing CNC from MCC. In previous study, with longer reaction time, the amount of dispersed CNC increased and reached almost 92% at 90 min reaction time (Fahma et al. 2010).

X-ray diffractometry (XRD)

To give more detailed information about the effect of chemical hydrolysis of MCC with different reaction time (30, 60, 90 and 120 min), the x-ray diffractometer was used to determine the crystallinity index of obtained CNC. Figure 2b shows the diffraction patterns obtained for CNC-1, CNC-2, CNC-3 and CNC-4. They are typical of cellulose I with four well-defined crystalline peaks around $2\Theta = 14$, 16, 22 and 34°. The XRD pattern of CNC-4 exhibited the most intense 200 peak and most resolved $1\bar{1}0$ and 110 peaks, indicating higher crystallinity index. Meanwhile, CNC-2 had the broadest and least defined XRD peaks among four samples (CNC-1, CNC-2, CNC-3 and CNC-4), a clear indication of lower crystallinity index. The crystallinity index of all samples were determined and the results are summarized in Table 4. The increased crystallinity index following 30 min dissolution time compared to the raw material (MCC) was ascribed to the progressive removal of amorphous materials. The crystallinity index calculated from XRD pattern of all samples were 73, 71, 75 and 76%, respectively.

Table 4 Crystallinity index of CNC at increased reaction time (CNC-1 = 30 min, CNC-2 = 60 min, CNC-3 = 90 min and CNC-4 = 120 min)

Sample	Crystallinity index (%)
MCC	60
CNC-1	73
CNC-2	71
CNC-3	75
CNC-4	76

However, the crystallinity index was slightly decreased from 73 to 71% as reaction time was increased to 60 min, supported by previous study (Fahma et al. 2010). In another study by Nguyen et al. (2010), as the reaction time endures to 8 h instead of 3 h, and the other conditions are unchanged, the crystallinity index was considerably reduced (Nguyen et al. 2010). This reducing crystallinity index was probably due to destructuring of crystalline structure at longer reaction time. As the reaction time was increased to 90 and 120 min, the crystallinity index was increased to 75 and 76% respectively, most probably because of the realignment of crystalline structure at longer reaction time. This XRD results together with the FTIR data confirmed that the CNC retained the cellulose I crystalline structure at different reaction times while becoming most crystalline at maximum reaction time. Compared to the study by Fahma et al. (2010), the crystallinity of CNC tended to decrease as the reaction time increases. This can be explained by the nature of acid used which cannot rapidly penetrate into the crystalline regions, because these regions are resistant to acid hydrolysis. In the process of cellulose hydrolysis, the amorphous regions are the first part attacked by acid. Despite the drastic conditions of hydrolysis, amorphous and crystalline regions may only be partially destroyed because of corrosion caused by the high concentration of sulfuric acid. As presented in Table 4, this study showed different, increasing crystallinity index trend despite longer reaction time. This study has then proved the advantages of using ILs instead of acid in controlling the hydrolysis of cellulose from occurring in the crystalline regions.

Thermogravimetric analysis (TGA)

TGA was measured to assess the thermal stability of CNC-1, CNC-2, CNC-3 and CNC-4 and the thermographs are presented in Fig. 3. They resemble the mass loss of the sample upon continuous heating up to 700 °C. Initial mass loss of all samples occur below 100 °C irrespective of their treatment. The initial change is attributed to the vaporisation of water because of the hydrophilic character of the samples. The mass loss was reliant on the initial moisture content of the analysed samples. Meanwhile, the second peak corresponded to the thermal disintegration of the cellulose (Deepa et al. 2011). As can be seen in Table 5, the onset temperature of CNC-1, CNC-2 and CNC-3, which indicates thermal stability, increased as the reaction time was increased.

In details, the DTG curve of sample hydrolysed at 60 and 90 min showed a minor increase in the degradation temperature (342 and 344 °C) respectively. The initial mass loss is a result of the presence of trace quantity of impurities in the CNC during the chemical treatment. However, no specific trend is observable from the mass loss occurred as seen in Table 5. Many studies were carried out to assess the decomposition of lignocellulosic materials. For example, (Yang et al. 2007) reported that in the thermal analysis, cellulose decomposition started at 315 °C and persisted until 400 °C. Maximum mass

Table 5 Thermal stability of CNC at increasing reaction time (CNC-1 = 30 min, CNC-2 = 60 min, CNC-3 = 90 min, CNC-4 = 120 min)

Sample	25–150 °C		150–700 °C			Residue mass (%)
	Mass loss (%)	T_1 (°C)	Onset (°C)	Mass loss (%)	Tmax (°C)	
CNC-1	1.5	60	330	90	350	8
CNC-2	2.1	60	342	90	375	8
CNC-3	1.8	60	344	83	375	15
CNC-4	1.6	60	280	85	375	13

loss rate was attained at 355 °C, while at 400 °C almost all cellulose was pyrolyzed, leaving small (6.5 wt%) solid residuals (Morán et al. 2008). The fibre residue that remains after heating all samples to 700 °C is a product of carbonization of the cellulosic materials in the inert atmosphere. As can be seen in Table 5, the residue at temperature around 700 °C in CNC-1, CNC-2, CNC-3 and CNC-4 were remarkably low which is at the range of 8–15 °C. It can be seen in Fig. 5 that no other degradation peaks were present except that of cellulose, which verified the conclusion that CNC samples prepared were very pure. The DSC and TGA results proved that the developed CNC have indeed enhanced thermal properties, making them less inclined to degradation and therefore can be processed at elevated temperatures. However, no significant relationship between the thermal stability and CrI of CNC-1, CNC-2, CNC-3 and CNC-4 can be concluded.

Atomic force microscopy (AFM)

The isolations of CNC were verified by means of AFM images, which was presented in Fig. 4b. The CNC had a rod-like aspect, individualized or agglomerated due to their high specific area and the strong hydrogen bonds established between crystallites. The average diameter, length and aspect ratio of CNC obtained is shown in Table 6. The CNC exhibited increased widths (9, 10, 21, 31 nm), decreased length (155, 146, 123, 80 nm) and aspect ratio (17, 15, 6, 3) with increasing reaction time.

The increasing trend of CNC dimension can be explained by the re-aggregation phenomenon. CNC tends to aggregate easily, forming a branch of cellulose or network-like cellulose. As longer time was given during the dissolution process, more aggregations will happen, resulting in bigger dimensions of CNC. To justify, the AFM images was shown in Fig. 4b, with maximum aggregations at longer reaction time. In contrast, the length of CNC decreased from 155 to 146 nm, 123 and 80 nm at longer reaction time. The decreasing length could be attributed by the efficiency of longer reaction time in breaking the cellulose chains. As more time given, more cleavage will happen resulting in shorter CNC, as supported by previous study (Fahma et al. 2010). Similar trend was also observed for the aspect ratio, whereby it decreased from 17 to 15, 6 and 3 respectively. Overall, the production of CNC was most efficient at minimum reaction time. In comparison with the previous studies, Bondeson et al. (2006) obtained larger CNC from MCC derived from Norway spruce, with a length between 200–400 nm and a width less than 10 nm. On the other hand, the CNC isolated from black spruce showed smaller and wider crystals, with a length of around 120 nm and a diameter of 4.9 nm, giving an aspect ratio of 24 (Beck-Candanedo et al. 2005). In the case of CNC isolated from the bark of Norway spruce, the average aspect ratio (L/D) was about 63, which is much higher than that of CNC isolated from wood (Le Normand et al. 2014). The aspect ratio of extracted CNC is also different from those extracted from coconut husks (35–44) (Rosa et al. 2010), sugarcane bagasse (32–64) (de Morais Teixeira et al. 2010), sisal (43–60) (Gutiérrez et al. 2008), regular cotton fiber (1014) (de Morais Teixeira et al. 2010), microcrystalline cellulose (11–13) (Capadona et al. 2009) and flax (Linum usitatissimum) (15) (Cao et al. 2009) (Morais et al. 2013). Still, the dimensions, length and aspect ratio of the CNC synthesized was within the accepted value, referring to all the previous data in these studies. However, an improvement in current method should be planned in order to increase the aspect ratio of the CNC.

Table 6 Diameter (nm), length (nm) and aspect ratio of CNC at increased reaction time (CNC-1 = 30 min, CNC-2 = 60 min, CNC-3 = 90 min and CNC-4 = 120 min)

Sample	Diameter (nm)	Length (nm)	Aspect ratio
CNC-1	9	155	17
CNC-2	10	146	15
CNC-3	21	123	6
CNC-4	31	80	3

Conclusions

CNC has been produced from MCC as starting materials, by using [Bmim][Cl]. When the reaction time was increased, the regeneration yield of CNC was gradually increased. Meanwhile, the crystallinity index and thermal stability of the CNC was first decrease, before increasing back at longer reaction time. Rod-like CNC that are 9–31 and 80–155 nm has been obtained. Meanwhile, as reaction temperature

was increased, the regeneration yield, crystallinity index, thermal stability, diameter and length of CNC were also increase. FTIR measurements of the CNC showed no derivational changes during the hydrolysis. Based on the results, increasing the reaction temperature and time exerted positive effect on the properties of CNC except re-aggregation phenomenon that occurred at higher reaction temperature and longer reaction time. After optimization study, the optimum temperature and reaction time were determined to be 100 °C and 30 min respectively, based on the highest value of aspect ratio (23, 17).

References

Beck-Candanedo S, Maren R, Gray DG (2005) Effect of reaction conditions on the properties and behaviour of wood cellulose nanocrystal suspensions. Biomacromol 6:1048–1054

Bondeson D, Mathew A, Oksman K (2006) Optimization of the isolation of nanocrystals from microcrystalline cellulose by acid hydrolysis. Cellulose 13(2):171–180. doi:10.1007/s10570-006-9061-4

Brinchi L, Cotana F, Fortunati E, Kenny JM (2013) Production of nanocrystalline cellulose from lignocellulosic biomass: technology and applications. Carbohyd Polym 94(1):154–169. doi:10.1016/j.carbpol.2013.01.033

Camacho F et al (1996) Microcrystalline-cellulose hydrolysis with concentrated sulphuric acid. J Chem Technol Biotechnol 67 (4):350–356

Cao Y et al (2009) Room temperature ionic liquids (RTILS): a new and versatile platform for cellulose processing and derivatization. Chem Eng J 147:13–21. doi:10.1016/j.cej.2008.11.011

Capadona JR, Shanmuganathan K, Trittschuh S, Seidel S, Rowan SJ, Weder C (2009) Polymer nanocomposites with nanowhiskers isolated from microcrystalline cellulose. Biomacromolecules 10(4):712–716

Cheng J-Y, Chu Y-H (2006) 1-Butyl-2,3-trimethyleneimidazolium bis(trifluoromethyl-sulfonyl)imide ([b-3C-im][NTf2]): a new, stable ionic liquid. Tetrahedron Lett 47:1575–1579. doi:10.1016/j.tetlet.2005.12.125

Deepa B et al (2011) Structure, morphology and thermal characteristics of banana nanofibers obtained by steam explosion. Bioresour Technol 102(2):1988–1997

de Morais Teixeira E, Corrêa AC, Manzoli A, de Lima Leite F, de Oliveira CR, Mattoso LHC (2010) Cellulose nanofibers from white and naturally colored cotton fibers. Cellulose 17(3):595–606

Fahma F et al (2010) Isolation, preparation, and characterization of nanofibers from oil palm empty-fruit-bunch (OPEFB). Cellulose 17:977–985. doi:10.1007/s10570-010-9436-4

Feng L et al (2008) Research progress on dissolution and functional modification of cellulose in ionic liquids. J Mol Liq 142(1–3):1–5. doi:10.1016/j.molliq.2008.06.007

Gutiérrez A, Rodriguez IM, Jose C (2008) Chemical composition of lipophilic extractives from sisal (*Agave sisalana*) fibers. Ind Crops Prod 28(1):81–87

Hong K, Zhang H, Mays JW, Visser AE, Brazel CS, Holbrey JD, Reichert WM, Rogers RD (2002) Conventional free radical polymerization in room temperature ionic liquids: a green approach to commodity polymers with practical advantages. Chem Commun 13(13):1368–1369

Hu X et al (2013) Functional ionic liquids for hydrolysis of lignocellulose. Carbohyd Polym 97(1):172–176

Le Normand M, Moriana R, Ek M (2014) Isolation and characterization of cellulose nanocrystals from spruce bark in a biorefinery perspective. Carbohyd Polym 111:979–987

Man Z et al (2011) Preparation of cellulose nanocrystals using an ionic liquid. J Polym Environ 19:726–731. doi:10.1007/s10924-011-0323-3

Mandal A et al (2011) Isolation of nanocellulose from waste sugarcane bagasse (SCB) and its characterization. Carbohyd Polym 86(3):1291–1299. doi:10.1016/j.carbpol.2011.06.030

Montalbo-Lomboy M, Grewell D (2015) Rapid dissolution of switchgrass in 1-butyl-3-methylimidazolium chloride by ultrasonication. Ultrason Sonochem 22:588–599. doi:10.1016/j.ultsonch.2014.06.013

Morán JI et al (2008) Extraction of cellulose and preparation of nanocellulose from sisal fibers. Cellulose 15(1):149–159

Morais JPS et al (2013) Extraction and characterization of nanocellulose structures from raw cotton linter. Carbohyd Polym 91(1):229–235. doi:10.1016/j.carbpol.2012.08.010

Nguyen TAD, Kim KR, Han SJ, Cho HY, Kim JW, Park SM, Park JC, Sim SJ (2010) Pretreatment of rice straw with ammonia and ionic liquid for lignocellulose conversion to fermentable sugars. Bioresource Technol 101(19):7432–7438

Olivier-Bourbigou H et al (2010) Ionic liquids and catalysis: recent progress from knowledge to applications. Appl Catal A 373(1–2):1–56. doi:10.1016/j.apcata.2009.10.008

Remsing RC, Swatloski RP, Rogers RD, Moyna G (2006) Mechanism of cellulose dissolution in the ionic liquid 1-n-butyl-3-methylimidazolium chloride: a 13 C and 35/37 Cl NMR relaxation study on model systems. Chem Commun 12(12):1271–1273

Rosa MF et al (2010) Cellulose nanowhiskers from coconut husk fibers: effect of preparation conditions on their thermal and morphological behavior. Carbohyd Polym 81 (1):83–92. doi:10.1016/j.carbpol.2010.01.059

Segal L et al (1959) An empirical method for estimating the degree of crystallinity of native cellulose using the X-ray diffractometer. Text Res J 29(10):786–794

Tan XY et al (2015) Preparation of high crystallinity cellulose nanocrystals (CNCs) by ionic liquid solvolysis. Biomass Bioenerg 81:584–591. doi:10.1016/j.biombioe.2015.08.016

Tian J et al (2010) Hydrolysis of cellulose by the heteropoly acid H3PW12O40. Cellulose 17(3):587–594

Yang H et al (2007) Characteristics of hemicellulose, cellulose and lignin pyrolysis. Fuel 86(12–13):1781–1788. doi:10.1016/j.fuel.2006.12.013

Yang D, Peng XW, Zhong LX, Cao XF, Chen W, Sun RC (2013) Effects of pretreatments on crystalline properties and morphology of cellulose nanocrystals. Cellulose 20 (5):2427–2437

Zhang H et al (2005) 1-Allyl-3-methylimidazolium chloride room temperature ionic liquid: a new and powerful non-derivatizing solvent for cellulose. Macromolecules 38 (20):8272–8277. doi:10.1021/ma0505676

Zhang J, Wang Y, Zhang L, Zhang R, Liu G, Cheng G (2014) Understanding changes in cellulose crystalline structure of lignocellulosic biomass during ionic liquid pretreatment by XRD. Biores Technol 151:402–405

Zhao H et al (2009) Regenerating cellulose from ionic liquids for an accelerated enzymatic hydrolysis. J Biotechnol 139:47–54. doi:10.1016/j.jbiotec.2008.08.009